Dynamics and thermodynamics in spinor quantum gases

H. Schmaljohann, M. Erhard, J. Kronjäger, K. Sengstock and K. Bongs

Institut für Laser-Physik, Universität Hamburg, Luruper Chaussee 149, 22761 Hamburg, Germany

February 2, 2008

Abstract

We discuss magnetism in spinor quantum gases theoretically and experimentally with emphasis on temporal dynamics of the spinor order parameter in the presence of an external magnetic field. In a simple coupled Gross-Pitaevskii picture we observe a dramatic suppression of spin dynamics due to quadratic Zeeman "dephasing". In view of an inhomogeneous density profile of the trapped condensate we present evidence of spatial variations of spin dynamics. In addition we study spinor quantum gases as a model system for thermodynamics of Bose-Einstein condensation. As a particular example we present measurements on condensate magnetisation due to the interaction with a thermal bath.

1 Introduction

The field of cold quantum gases has seen a rapid growth since the first realisation of Bose-Einstein condensation in dilute atomic gases in 1995 [1, 2, 3] accompanied with the development of a broad range of tools for the detailed control of these systems. Single component Bose-Einstein condensates have evolved into a fundamental model system showing many intriguing phenomena. For an overview see e.g. [4, 5, 6, 7, 8, 9, 10, 11]. In contrast to these systems with a scalar order parameter spinor Bose-Einstein condensates offer spin as a new degree of freedom and are consequently represented by a vector order parameter. In addition to being mixtures of different bosonic species the different components in these multicomponent quantum systems are coupled and can exchange particles. This makes spinor Bose-Einstein condensates unique systems, which on the one hand possess intrinsic magnetic properties and on the other hand give access to well controlled Bose-Einstein thermodynamics with adjustable heat and particle bath.

Magnetism in degenerate quantum gases offers new regimes for studies of collective spin phenomena [12, 13, 14, 15, 16, 17, 18, 19, 20, 21, 22, 23, 24, 25, 26, 27, 28] and opens new perspectives in view of the closely related entangled spin systems in atomic quantum gases, which show intriguing prospects for quantum optics and quantum computation [29, 30, 31, 32, 33].

So far studies concentrated on the magnetic properties of spin 1 ultracold quantum gases in optically trapped ^{23}Na [22, 23, 24, 26] and recently in ^{87}Rb [34, 27, 28, 35], where also the intrinsically more complex F=2 spin state became accessible [27, 35].

Systems closely related to these spinor condensates are effective spin-1/2 systems realized by radiofrequency coupling of two hyperfine states in ^{87}Rb [19, 20, 21], in which spin-waves [25] and decoherence effects were observed [36].

In this paper we will concentrate on F=1 and F=2 spinor condensates of ^{87}Rb in two limits. First we investigate the coherent spinor evolution of a trapped ensemble at zero temperature in the presence of a homogeneous magnetic field, where we find suppression of spin dynamics due to the quadratic Zeeman effect as well as a spatial depedence of the dynamics. The other limit is thermally dominated spin dynamics at temperatures close to T_c, where a significant fraction of the atoms occupies the normal component. Spinor gases in this regime can act as a versatile model system for thermodynamics with tunable heat and particle bath as recently demonstrated with a constant temperature Bose-Einstein phase transition [37]. In this paper we will present new data on thermally induced condensate magnetisation as another intriguing example of spinor thermodynamics.

2 Spinor condensates at T=0

The theory presented in this section is based on a mean field approach, in extension of the very successful treatment of single component Bose-Einstein condensates. The basic two-particle interactions are represented by a density and spin-composition dependent average energy shift. This approach has first been developed for F=1 systems [12, 13] and was later extended to F=2 systems [15, 18].

For typical experimental parameters the mean field shifts connected to collisions in different spin channels dominate magnetic dipole dipole interactions by at least one order of magnitude. In the following analysis magnetic dipole dipole interactions will thus be neglected. The intrinsic dynamics of a spinor condensate is determined by a pairwise interaction potential [12, 15]:

$$\hat{V}(\mathbf{r_1} - \mathbf{r_2}) = \delta(\mathbf{r_1} - \mathbf{r_2}) \sum_{f=0}^{2F} \frac{4\pi\hbar^2 a_f}{m} \hat{P}_f. \qquad (1)$$

Here a_f denotes the s-wave scattering length for a collision channel of two particles whose single spins F are combined to give the total spin f, $\hat{P}_f$ is the corresponding projection operator onto total spin f and m is the mass of a single atom. Due to Bose symmetry only even total spin channels (e.g. a_0, a_2, a_4 for $F = 2$) are involved with the maximum total spin given by

$f = 2F$. Making use of the relation $\left(\vec{F}_1 \cdot \vec{F}_2\right)^n = \sum_{f=0}^{2F} \lambda_f^n P_f$ with $\lambda_f = \frac{1}{2}\left[f(f+1) - 2F(F+1)\right]$ the projection operators can be replaced by spin expectation values [12].

In the following we will concentrate on the case $F = 1$ for the theoretical considerations in order to point out some important aspects of spin dynamics, which are straightforward to extend to the $F = 2$ case.

In second quantised form the Hamiltonian for a $F = 1$ system at zero magnetic field is given by [12]:

$$H = \int d^3r \left(\frac{\hbar^2}{2m}\nabla\psi_a^\dagger \cdot \nabla\psi_a + V_{ext}\psi_a^\dagger\psi_a \right.$$
$$+\frac{g_0}{2}\psi_a^\dagger\psi_{a'}^\dagger\psi_{a'}\psi_a$$
$$\left. +\frac{g_2}{2}\psi_a^\dagger\psi_{a'}^\dagger\vec{\mathbf{F}}_{\mathbf{ab}}\cdot\vec{\mathbf{F}}_{\mathbf{a'b'}}\psi_{b'}\psi_b\right). \qquad (2)$$

In this expression $\psi_a(\vec{r})$ is the field annihiliation operator for an atom in state $m_F = a$ at point $\vec{r}$ and V_{ext} is the trapping potential. The spin-independent mean-field interaction is parameterised by $g_0 = \frac{2\pi\hbar^2}{m} \times \frac{2a_2+a_0}{3}$. The spin-dependent mean-field responsible for the systems magnetic properties is characterised by the parameter $g_2 = \frac{4\pi\hbar^2}{m} \times \frac{a_2-a_0}{3}$ and the coupling between different states is determined by the spin-matrices:

$$F_x = \frac{1}{\sqrt{2}}\begin{pmatrix} 0 & 1 & 0 \\ 1 & 0 & 1 \\ 0 & 1 & 0 \end{pmatrix}, \quad F_y = \frac{i}{\sqrt{2}}\begin{pmatrix} 0 & -1 & 0 \\ 1 & 0 & -1 \\ 0 & 1 & 0 \end{pmatrix}, \quad (3)$$

$$F_z = \begin{pmatrix} 1 & 0 & 0 \\ 0 & 0 & 0 \\ 0 & 0 & -1 \end{pmatrix} \quad (4)$$

From the spin matrices it follows, that for F=1 spinor condensates the only coupling process is between states with $m_F = 0$ and $m_F = \pm 1$ and that the total spin projection is preserved by the interaction. It is important to emphasise this again to demonstrate that the total spin in a finite atomic quantum gas system is conserved, in contrast to a homogeneous infinite system and in contrast to many condensed matter systems. Therefore the actual ground state of the system depends on the initial magnetisation.

For macroscopically occupied Bose-systems at $T = 0$ it is common to replace the field annihilation operators by their expectation value, i.e. $\varphi_a(\vec{r},t) \equiv \langle\psi_a(\vec{r},t)\rangle$, which for spinor condensates is conveniently expressed as [12]

$$\varphi_a(\vec{r},t) = \sqrt{n(\vec{r},t)}e^{i\phi(\vec{r},t)}\zeta_a(\vec{r},t). \qquad (5)$$

Here $n(\vec{r},t)$ is the condensate density, $\phi(\vec{r},t)$ a phase and $\vec{\zeta}(\vec{r},t) = (\zeta_{+1}, \zeta_0, \zeta_{-1})^T$ is a normalized spinor with $\vec{\zeta}^\dagger \cdot \vec{\zeta} = 1$.

Using (5), neglecting the density dependence on the spin state and adding the effect of a weak magnetic field one gets the following system of differential equations for the evolution of an F=1 spinor condensate:

$$i\hbar\frac{\partial}{\partial t}\sqrt{n(\vec{r},t)}e^{i\phi(\vec{r},t)} = \left(-\frac{\hbar^2\nabla^2}{2m} + V_{ext.}(\vec{r}) + g_0 n(\vec{r})\right)$$
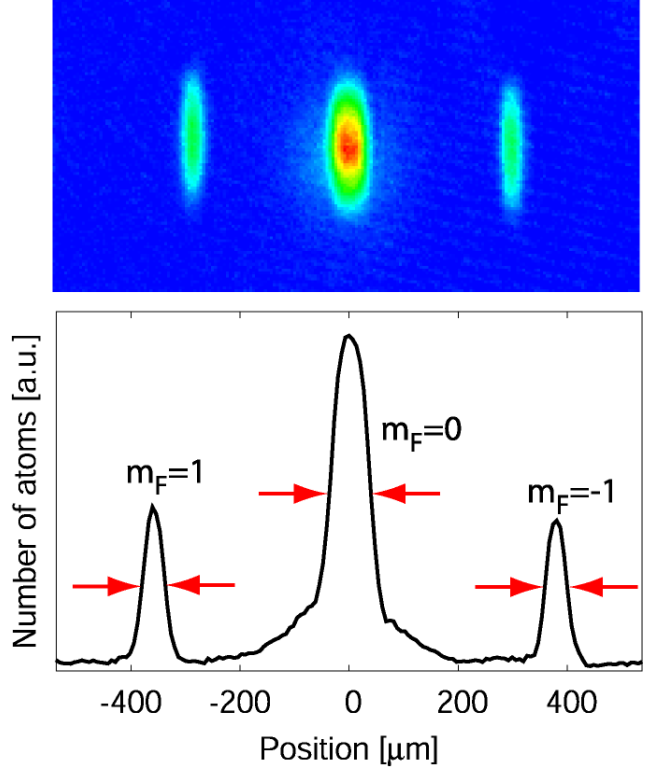$$\cdot \sqrt{n(\vec{r},t)}e^{i\phi(\vec{r},t)}, \qquad (6)$$

Figure 1: Absorption images and vertically summed cross sections of a spinor condensate after $10\,\mathrm{ms}$ evolution starting with the initially prepared state $F = 2$, $m_F = 0$. The images were taken after a combined time of flight and Stern Gerlach separation, leading to a rapid radial expansion and a separation of the different spinor components. The graphs clearly show a reduced width in the axial distribution of the $m_F = \pm 1$ components created by spin dynamics in the high density center of the $m_F = 0$ component.

$$i\hbar\frac{\partial}{\partial t}\vec{\zeta}(\vec{r},t) = -\frac{\hbar^2 n(\vec{r},t)\nabla^2}{2m}\vec{\zeta}(\vec{r},t)$$
$$+g_2 n(\vec{r},t)\vec{\mathcal{F}}\vec{\zeta}(\vec{r},t)\vec{\zeta}^\dagger(\vec{r},t)\vec{\mathcal{F}}\vec{\zeta}(\vec{r},t)$$
$$-p\mathcal{F}_z\vec{\zeta}(\vec{r},t) + q(\mathcal{F}_z^2 - 4)\vec{\zeta}(\vec{r},t). (7)$$

From these equations it follows, that spin dynamics (represented by the terms containing $\vec{\mathcal{F}}$) is proportional to $g_2 n(\vec{r},t)$, i.e. the local density. This has important consequences for the usual experimental situation of trapped samples, having an inhomogeneous density distribution. Two regimes can be identified: 1. the spin dynamics rates are higher than one or more trapping frequencies and 2. spin dynamics is slow compared to trap dynamics. In the first case there will be a significant coupling between spin dynamics and motional dynamics, while the second case is comparable to the homogeneous density case. As was shown for the first time in [27] ^{87}Rb has the fascinating properties that it offers fast spin dynamics in the F=2 state (on the order of a few ms) and slow spin dynamics in the F=1 state (on the order of a few s). Therefore also different spatial regimes can be thought of with ^{87}Rb spinor condensates.

Fig. 1 shows the initial evolution of an F=2 ^{87}Rb spinor

condensate prepared in the $m_F = 0$ spin state with a central density $n \approx 4 \cdot 10^{14}\,\mathrm{cm}^{-3}$. In this case spin dynamics takes place with timescales on the order of a few ms [27], faster than the axial trap dynamics characterised by a frequency of $\approx 21\,\mathrm{Hz}$. The other trapping frequencies of $\approx 155\,\mathrm{Hz}$ and $\approx 890\,\mathrm{Hz}$ imply motional dynamics faster than the spin evolution and are thus neglected in the following. The image in Fig. 1 was taken after switching off the trapping potential and 31 ms time of flight during which a magnetic field gradient was applied for 5 ms to achieve a Stern-Gerlach separation of the spinor components. The axial trap direction was horizontal, along which only weak mean field induced expansion takes place during time of flight. The vertically summed horizontal cross sections shown in Fig. 1 thus approximately represent the axial distribution of the trapped sample. The images and graphs clearly demonstrate the density dependence of spin dynamics, as the $m_F = \pm 1$ spin states show a smaller width than the "mother" $m_F = 0$ component. This is due to the parabolic density profile of the "mother" component, which implies a fast spin state conversion in the center of the trap. Very recently a spatial dependence in ^{87}Rb (F=2) condensate spin dynamics was also observed in [35]. Further investigations of the coupled spin and spatial dynamics were limited in our case by the finite optical resolution and will be subject to future investigations.

Interestingly external magnetic fields are a further additional parameter to control spin dynamics. Whereas most theoretical work so far concentrated on the physics at B=0, experiments [24, 27, 28, 35] clearly demonstrated the importance of extermal field influences. Magnetic fields can completely hinder spin dynamics or on the other hand strongly stimulate dynamics. In the following we will mainly concentrate on a discussion of spin dynamics suppression due to the quadratic Zeeman effect. Very recently the suppression of spin dynamics in F=2 spinor condensates was experimentally observed in [35]. The following discussion can explain these observations in their main part.

The magnetic field enters equations (7) via the linear Zeeman shift as well as the quadratic Zeeman shift with the coupling constants $p = g_F \mu_B B$ and $q = -\frac{\mu_B^2 B^2}{4\hbar\omega_{12}}$ with ω_{12} representing the hyperfine splitting. As we will see later the relatively large linear Zeeman energy $(q/B \approx k_B \cdot 34\mu\mathrm{K/G})$ does not influence the spin dynamics, which in fact is due to total spin conservation. This is not true for the quadratic Zeeman effect! For typical experimental conditions with off-set fields of several $100\,\mathrm{mG}$ the quadratic Zeeman energy $(|q|/B^2 \approx k_B \cdot 3.5\,\mathrm{nK/G}^2)$ can reach values comparable to the intrinsic spin coupling (on the order of k_B times one nK for typical condensate densities of a few $10^{14}\,\mathrm{cm}^{-3}$).

In order to extract the basic influence of the quadratic Zeeman effect on spin dynamics, we assume a homogeneous case with constant $n(\vec{r}, t) = n$ and no spatial spin variation $\vec{\zeta}(\vec{r}, t) = \vec{\zeta}(t)$. With these assumptions equation (7) reads

$$i\hbar\frac{\partial}{\partial t}\zeta_{+1} = g_2 n \left(\zeta_{+1}^* \zeta_{+1}\zeta_{+1} + \zeta_0^*\zeta_{+1}\zeta_0 - \zeta_{-1}^*\zeta_{+1}\zeta_{-1} \right.$$
$$\left. + \zeta_{-1}^*\zeta_0^2\right) - p\zeta_{+1} - 3q\zeta_{+1},$$

$$i\hbar\frac{\partial}{\partial t}\zeta_0 = g_2 n \left(\zeta_{+1}^*\zeta_{+1}\zeta_0 + \zeta_{-1}^*\zeta_0\zeta_{-1} + 2\zeta_0^*\zeta_{+1}\zeta_{-1}\right)$$
$$- 4q\zeta_0, \tag{8}$$

$$i\hbar\frac{\partial}{\partial t}\zeta_{-1} = g_2 n \left(\zeta_{-1}^*\zeta_{-1}\zeta_{-1} - \zeta_{+1}^*\zeta_{+1}\zeta_{-1} + \zeta_0^*\zeta_0\zeta_{-1}\right.$$
$$\left. + \zeta_{+1}^*\zeta_0^2\right) + p\zeta_{-1} - 3q\zeta_{-1}.$$

Using a simple change of variables

$$\lambda_{\pm 1} = \zeta_{\pm 1}\,\exp(\mp i(p \pm 3q)t/\hbar)$$
$$\text{and} \tag{9}$$
$$\lambda_0 = \zeta_0\,\exp(-i4qt/\hbar),$$

the linear Zeeman dependence is removed from the equations and the quadratic Zeeman effect enters in a more symmetric way:

$$i\hbar\frac{\partial}{\partial t}\lambda_{+1} = g_2 n \left(\lambda_{+1}^*\lambda_{+1}\lambda_{+1} + \lambda_0^*\lambda_{+1}\lambda_0 - \lambda_{-1}^*\lambda_{+1}\lambda_{-1}\right.$$
$$\left. + \lambda_{-1}^*\lambda_0^2 e^{i2qt/\hbar}\right),$$

$$i\hbar\frac{\partial}{\partial t}\lambda_0 = g_2 n \left(\lambda_{+1}^*\lambda_{+1}\lambda_0 + \lambda_{-1}^*\lambda_0\lambda_{-1}\right.$$
$$\left. + 2\lambda_0^*\lambda_{+1}\lambda_{-1}e^{-i2qt/\hbar}\right), \tag{10}$$

$$i\hbar\frac{\partial}{\partial t}\lambda_{-1} = g_2 n \left(\lambda_{-1}^*\lambda_{-1}\lambda_{-1} - \lambda_{+1}^*\lambda_{+1}\lambda_{-1} + \lambda_0^*\lambda_0\lambda_{-1}\right.$$
$$\left. + \lambda_{+1}^*\lambda_0^2 e^{i2qt/\hbar}\right).$$

In these equations derived here spin exchange is described by the terms with exponentials, while the other terms represent the mean field phase evolution. Fig. 2 shows the relative spinor occupations and the relative phase $\phi_{+1} - 2\phi_0 + \phi_{-1}$ as a result of a numerical simulation of equations (10) for different magnetic offset fields. The spin component phases are given by $\phi_i = \arg(\lambda_i)$ with the phase $\phi_{+1} - 2\phi_0 + \phi_{-1}$ is the relevant phase for the evolution of the $m_F = 0$ component. The initial conditions were chosen symmetric with density $n = 4 \cdot 10^{14}\,\mathrm{cm}^{-3}$, $|\lambda_0| = 0.9$, $|\lambda_{\pm 1}| = 0.05$ and $\phi_i(t = 0) = 0$.

The numerical simulation clearly shows that the quadratic Zeeman effect strongly suppresses spin dynamics if it is larger than the spin dependent mean field shifts. For ^{87}Rb in F=1 and at densities of a few times $10^{14}\,\mathrm{cm}^{-3}$ this suppression becomes relevant at magnetic fields of a few $100\,\mathrm{mG}$.

The suppression of spin dynamics at high magnetic fields can also be directly deduced analysing the expression for λ_0, which according to equation (10) at high magnetic fields will approximately evolve due to the rapidly changing exponential giving:

$$\lambda_0(t_{final}) \approx \lambda_0(t_0)$$
$$- \left[\frac{g_2 n}{2q}\lambda_0^*(t_0)\,\lambda_{-1}(t_0)\,\lambda_{+1}(t_0)\,e^{-i2qt/\hbar}\right]_{t_0}^{t_{final}} \tag{11}$$

If $q \gg g_2 n$ there will be nearly no change in the occupation of spin states as predicted by the numerical simulation.

In summary (in the absence of a field gradient) the linear Zeeman effect can be neglected for investigations on spin dynamics in spinor Bose condensates due to the always symmetric exchange of Zeeman energy (Fig. 3a), which is fundamentally caused by spin conservation. In contrast we found that
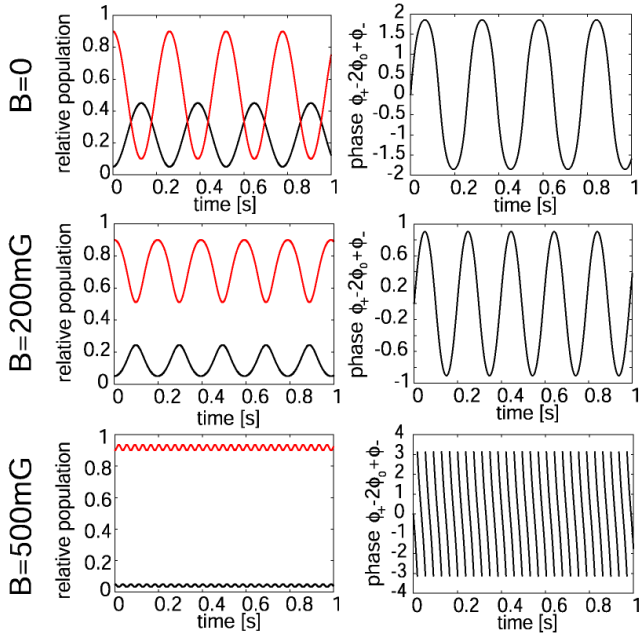
Figure 2: Numerical simulation of equations (10) for different magnetic field strengths. The graphs on the left show the evolution of the population of spin state $m_F = 0$ (red) and of spin states $m_F = \pm 1$ (black). The graphs on the right show the evolution of the relative phase corresponding to the interaction $2|0\rangle \leftrightarrow |1\rangle + |-1\rangle$. A strong reduction of the amplitude of the oscillation in the spin populations for higher magnetic fields is clearly visible.
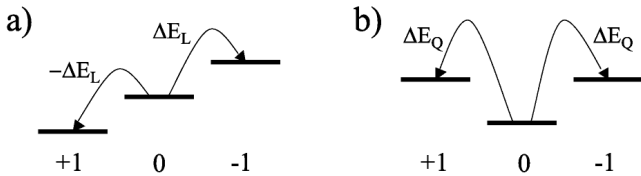

Figure 3: Schematic view of F=1 ($|1\rangle + |-1\rangle \leftrightarrow 2|0\rangle$) spin dynamics with additional magnetic field. The different m_F states are labeled by 0 and ± 1. (a) The total linear Zeeman energy is conserved in spin dynamics as the energy gain in one component is lost in the other. (b) The quadratic Zeeman shifts (shown with the linear Zeeman contribution subtracted and rescaled as typically $\Delta E_Q \ll \Delta E_L$) however lead to an energy imbalance in spin dynamics.

spin dynamics can be significantly altered by the quadratic Zeeman effect, where an additive energy exchange (Fig. 3b) leads to a "dephasing" of the spin components ultimately stopping spin dynamics at high magnetic fields. One could say that high external magnetic fields "pin" the spin to its value. Intrinsic spin dynamics can be observed up to magnetic fields for which $q(B) \simeq g_2 n$ typically corresponds to fields of a few $100\,\mathrm{mG}$. We want to emphasize that the blocking of spin dynamics is solely due to the quadratic Zeeman effect and does not follow energetical considerations. Indeed with this blocking effect we can explain the experimentally observed high magnetic field suppression of spin dynamics even when it is leading to an energetically lower state [35].

Furthermore we found evidence of spatially varying spin dynamics in trapped spinor condensates with inhomogeneous density. This effect will lead to complex coupled dynamics of spatial and spin degrees of freedom to be investigated in future experiments.

3 Thermodynamics with spinor condensates

Finite temperature effects in Bose-Einstein condensates represent an active area of research, which is still relatively unexplored due to its theoretical complexity and experimental challenges. In theory sophisticated methods have been developed to reduce the complexity of simulations such that modelling complex phenomena seems feasible [38, 39, 40, 41, 42]. Major tests for these models consisted in the interpretation of early experiments on damping of single component condensate excitations in the presence of a normal component and on condensate formation.

Spinor condensates offer a novel approach to well controlled Bose-Einstein thermodynamics. As a first aspect they are multicomponent systems such that a thermal bath for one component can easily be created by tailoring the other component(s). This aspect is widely used in sympathetic cooling experiments with multi-species mixtures. Spinor multicomponent systems add the essential aspect of particle exchange between the components, which is required to complete thermodynamics. The particle exchange takes place due to intrinsic interparticle interactions but can also be experimentally controlled via additional external electromagnetic fields. These aspects and the relevant interactions with respect to thermodynamics in spinor quantum gases are shown schematically in Fig. 4.

An important point in the study of spinor systems is connected to the coherence between different spin components. Coherent spin mixtures, i.e. mixtures in which each single atom (in the normal component as well as in the condensate fraction) is in the same quantum superposition of spin states, are effectively single component quantum gases, which have to be contrasted to incoherent spin mixtures, where different spin states represent different species gases. For example if a F=1 spinor gas in the first case would be described by N particles in a spin superposition state $\phi = \alpha|1\rangle + \beta|0\rangle + \gamma|-1\rangle$ then the incoherent state would be given by a mixture of three
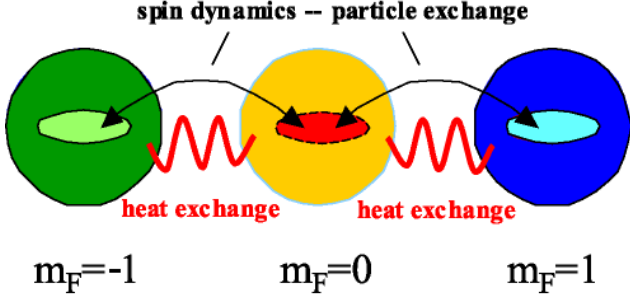
Figure 4: Schematic view of thermodynamics in spinor quantum gases for the example of a spin F=1 system. In this example the states with $m_F = 1 = |1\rangle$ and $m_F = -1 = |-1\rangle$ act as a heat bath and particle reservoir for the state $m_F = 0 = |0\rangle$. Heat (energy) is exchanged by elastic collision processes involving atoms in the normal component. Particles are exchanged in spin-changing collisions via the interaction $|1\rangle + |-1\rangle \leftrightarrow 2|0\rangle$. An important aspect of particle exchange lies in the density dependence of spin dynamics, which nearly exclusisively takes place in the dense condensate fraction. Particle exchange thus involves only small energy transfer and does practically not contribute to thermalization processes. Spinor condensates thus allow to create systems with independently tunable particle and heat exchange.
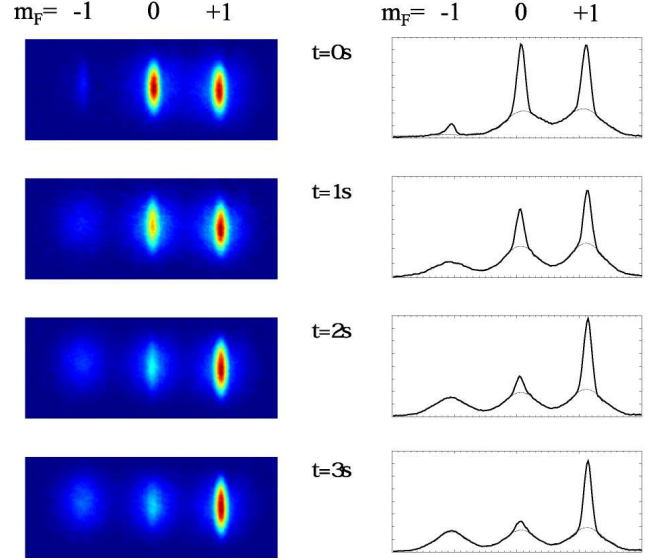

Figure 5: Absorption images and cross sections showing the temporal evolution of a spinor condensate prepared in the states $m_F = 1$ and $m_F = 0$ with a significant fraction of atoms in the normal cloud (the initial population in $m_F = -1$ is due to slight preparation imperfections).

gases, one with $N_1 = |\alpha|^2$ particles in the $|1\rangle$ state, one with $N_0 = |\beta|^2$ particles in the $|0\rangle$ state and one with $N_{-1} = |\gamma|^2$ particles in the $|-1\rangle$ state.

Indeed incoherent spin mixtures are in some cases of high experimental importance, e.g. for the conversion of two spin state fermion mixtures to a molecular Bose gas with a Feshbach resonance. This was nicely demonstrated and explained in [43] for the preparation of a spin state mixture in ^{6}Li. As an another example the distinction between coherent and incoherent spin superpositions is crucial to the understanding of the recently demonstrated decoherence driven cooling [36] in a quasi spin 1/2 system.

The evolution of F=1 and F=2 spinor condensates discussed in this paper can be tuned in between the regimes of coherent and incoherent evolution by adapting the parameters temperature, density and possibly external radiofrequency coupling. An intriguing example for mostly coherent evolution is the observation of spinor oscillations [27, 28, 35]. The incoherent limit was recently reached in a thermalization dominated regime with the demonstration of constant temperature Bose-Einstein condensation [37] in F=1 spinor condensates with significant occupation in the normal component.

In the following we will further concentrate on the thermalization dominated regime in F=1 ^{87}Rb and investigate the evolution of an initially prepared $|1\rangle + |0\rangle$ mixture (see Fig. 5).

Due to total spin conservation the only spin dynamics is the coupling $2|0\rangle \leftrightarrow |1\rangle + |-1\rangle$, which in this case initially leads to the depletion of the $|0\rangle$ state in favor of the (initially already populated) $|1\rangle$ and the (initially empty) $|-1\rangle$ states. As spin

dynamics is mostly occurring in the condensate fraction, low energy atoms are added to the $|1\rangle$ and $|-1\rangle$ states, which in the case of the $|1\rangle$ state just add to the condensate fraction (the particle number in the normal component of this state is saturated for the given temperature). The case of the newly populated $|-1\rangle$ state is however significantly different, as this state does not yet possess a normal component. The low energy atoms in this state quickly (on a shorter timescale - on the order of 50 ms than spin dynamics - on the order of seconds) thermalise with the normal component atoms of the other spin states. This leads to a slow buildup of the $|-1\rangle$ normal component and at the same time an increase in condensate fraction in the $|1\rangle$ component, while the $|0\rangle$ state condensate fraction decreases.

An interesting point is that this process leads to a slight decrease in temperature, as it uses energy from the existing normal components to thermalise the low energy atoms entering the $|-1\rangle$ state from the $|0\rangle$ condensate fraction. This temperature decrease at the expense of total condensate fraction is similar to decoherence driven cooling observed in quasi spin 1/2 systems [36].

We want to emphasise that under typical experimental conditions the thermal energy corresponds to roughly $k_B \times 300$ nK and is thus more than an order of magnitude larger than the spin dependent mean-field shifts of roughly $k_B \times 10$ nK responsible for spin dynamics. This directly implies that in thermal equilibrium the normal components of different spin states will have equal population (if there are sufficiently many atoms available in each spin component). For the case discussed in this paper the $|-1\rangle$ normal component will grow until either the $|0\rangle$ condensate fraction is completely depleted or it reaches its saturated occupation for the given tempera-
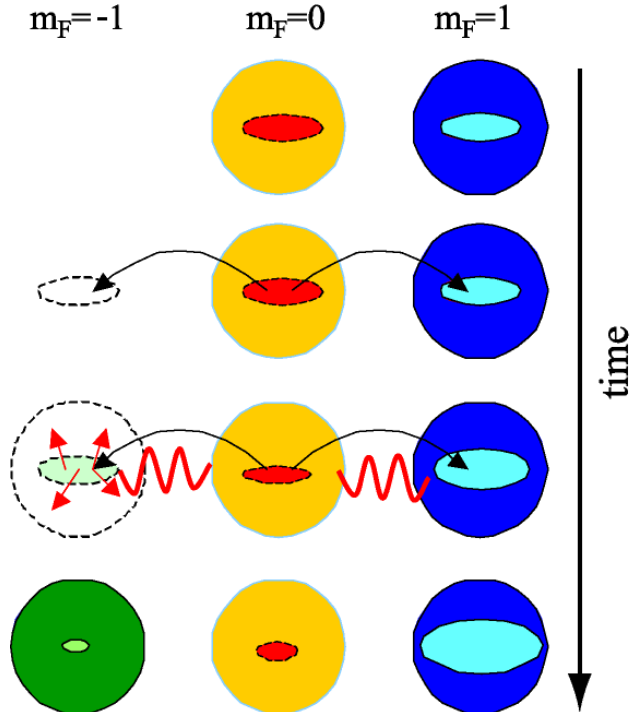
Figure 6: Schematic view of condensate magnetisation in thermally dominated spin dynamics. The top row shows the initially prepared state. Spin dynamics is transferring population from the $|0\rangle$ condensate fraction to the $\pm 1\rangle$ condensate fractions (second row). Due to fast thermalisation and the absence of a $|-1\rangle$ normal component, the new $|-1\rangle$ atoms start to populate the normal component, while the new $|+1\rangle$ just add to the corresponding condensate fraction (third row). In the end there will be thermal equilibrium with equally populated normal components (zero total spin) and a stronger than initial condensate fraction magnetisation.

ture, i.e. the same occupation as the other spin state normal components (which are saturated, as there exists a condensate fraction in these components). Only in the second case a condensate fraction will build up in the $|-1\rangle$ state, which now will be determined not by the thermal energy scale but by spin dynamics [37].

In any case this process will tend towards a total zero spin in the normal components (equal occupation) and thus shift the total spin of the condensate fractions towards more positive values. The strongest magnetisation of the condensate fraction occurs if the initial population of the $|0\rangle$ condensate fraction does not suffice to saturate the $|-1\rangle$ normal component occupation via spin dynamics. In this case spin dynamics stops after the $|0\rangle$ condensate fraction is depleted and only a $|+1\rangle$ condensate fraction remains, i.e. the condensate fraction is fully magnetised.

The principle mechanisms are again summarized in Fig. 6: The population of the $|-1\rangle$ condensate part thermalises and fills up a $|-1\rangle$ normal component. Thus the normal conponent total spin finally adds up to zero. Due to spin conservation, the condensate spin has to increase, which is reflected in a
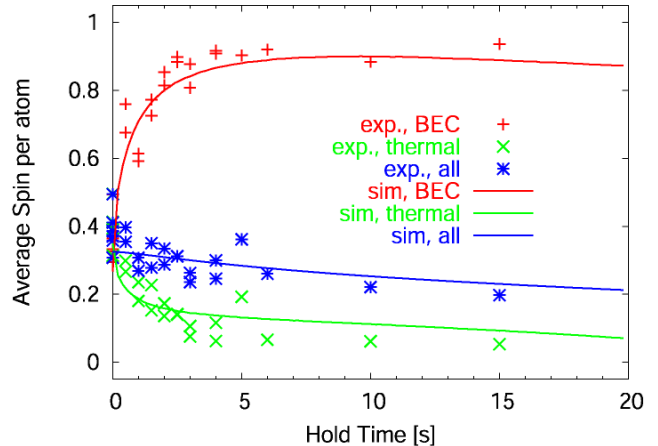

Figure 7: Experimental data versus a simulation for thermally dominated spinor dynamics for an initial preparation of the sample in $m_F = 1$ and $m_F = 0$. The graph shows the average magnetisation of atoms in the condensate fraction, atoms in the normal fraction and in total.

higher $|+1\rangle$ condensate fraction population. This process is clearly reflected in the experimental data presented in Fig. 7. The data is well reproduced by a numerical simulation based on a simple rate equation model, presented in detail in [37]. The slight decrease in the average spin for the total ensemble is due to the fact that the trap losses are dominated by three body collisions, predominantly occurring in the magnetised condensate fraction.

In conclusion in this paper we have presented investigations on spatial variations, influence of magnetic fields and high temperature as fundamental and new aspects in spinor dynamics. We found that fast spin dynamics in inhomogeneous (trapped) ensembles leads to spatial effects which promises new complex coupled spatial and spin dynamics. We have shown, that the dominant magnetic field influence stems from the quadratic Zeeman effect, limiting the offset fields up to which spinor dynamics can be observed for typical experimental conditions to a few $100\,\mathrm{mG}$. Furthermore we investigated the regime of finite temperature spinor dynamics considering the example of condensate magnetisation in favour of an equalised spin distribution in the normal component. This work demonstrates the versatility and complexity of spinor Bose-Einstein condensates and paves the way for a broad range of future investigations.

References

[1] M. H. Anderson, J. R. Ensher, M. R. Matthews, C. E. Wieman, and E. A. Cornell. Observation of Bose-Einstein condensation in a dilute atomic vapor. *Science*, 269(0):198, 1995.

[2] K. B. Davis, M.-O. Mewes, M. R. Andrews, N. J. van Druten, D. S. Durfee, D. M. Kurn, and W. Ketterle.

Bose-Einstein condensation in a gas of sodium atoms. *Phys. Rev. Lett.*, 75(22):3969, 1995.

[3] C. C. Bradley, C. A. Sackett, J. J. Tollett, and R. G. Hulet. Evidence of Bose-Einstein condensation in an atomic gas with attractive interactions. *Phys. Rev. Lett.*, 75(9):1687, 1995. *ibid.* **79**, 1170 (1997).

[4] E. A. Cornell, J. R. Ensher, and C. E. Wieman. Experiments in dilute atomic Bose-Einstein condensation. In M. Inguscio, S. Stringari, and C. E. Wieman, editors, *Proceedings of the International School of Physics - Enrico Fermi*, page 15. IOS Press, 1999.

[5] W. Ketterle, D. S. Durfee, and D. M. Stamper-Kurn. Making, probing and understanding Bose-Einstein condensates. In M. Inguscio, S. Stringari, and C. E. Wieman, editors, *Proceedings of the International School of Physics - Enrico Fermi*, page 67. IOS Press, 1999.

[6] F. Dalfovo, S. Giorgini, L. P. Pitaevskii, and S. Stringari. Theory of Bose-Einstein condensation in trapped gases. *Rev. Mod. Phys.*, 71(3):463, 1999.

[7] Ph. W. Courteille, V. S. Bagnato, and V. I. Yukalov. Bose-Einstein condensation of trapped atomic gases. *Laser Phys.*, 11.

[8] C. J. Pethick and H. Smith. *Bose-Einstein Condensation in Dilute Gases.* Cambridge University Press, 2002.

[9] L. P. Pitaevskii and S. Stringari. *Bose-Einstein Condensation (The International Series on Monographs on Physics.* Oxford University Press, 2003.

[10] J. O. Andersen. Theory of the weakly interacting Bose gas. *cond-mat/*, 0305138, 2003.

[11] K. Bongs and K. Sengstock. Physics with coherent matter waves. *Rep. Prog. Phys.*, 67:907, 2004.

[12] Tin-Lun Ho. Spinor Bose condensates in optical traps. *Phys. Rev. Lett.*, 81(4):742, July 1998.

[13] T. Ohmi and K. Machida. Bose-Einstein condensation with internal degrees of freedom in alkali atom gases. *J. Phys. Soc. Jpn.*, 67:1822, 1998.

[14] Tomoya Isoshima, Kazushige Machida, and Tetsuo Ohmi. Spin-domain formation in spinor Bose-Einstein condensation. *Phys. Rev. A*, 60(6):4857, December 1999.

[15] M. Koashi and M. Ueda. Exact eigenstates and magnetic response of spin-1 and spin-2 Bose-Einstein condensates. *Phys. Rev. Lett.*, 84:1066, 2000.

[16] Tin-Lun Ho and Lan Yin. General structure of Bose-Einstein condensates with arbitrary spin. *Phys. Rev. Lett.*, 84(11):2302, March 2000.

[17] Tin-Lun Ho and Sung Kit Yip. Fragmented and single condensate ground states of spin-1 Bose gas. *Phys. Rev. Lett.*, 84(18):4031, May 2000.

[18] C. V. Ciobanu, S.-K. Yip, and Tin-Lun Ho. Phase diagrams of $F{=}2$ spinor Bose-Einstein condensates. *Phys. Rev. A*, 61:033607, February 2000.

[19] C. J. Myatt, E. A. Burt, R. W. Ghrist, E. A. Cornell, and C. E. Wieman. Production of two overlapping Bose-Einstein condensates by sympathetic cooling. *Phys. Rev. Lett.*, 78(4):586, January 1997.

[20] D. S. Hall, M. R. Matthews, J. R. Ensher, C. E. Wieman, and E. A. Cornell. Dynamics of component separation in a binary mixture of Bose-Einstein condensates. *Phys. Rev. Lett.*, 81(8):1539, August 1998.

[21] M. R. Matthews, D. S. Hall, D. S. Jin, J. R. Ensher, C. E. Wieman, E. A. Cornell, F. Dalfovo, C. Minniti, and S. Stringari. Dynamical response of a Bose-Einstein condensate to a discontinuous change in internal state. *Phys. Rev. Lett.*, 81(2):243, July 1998.

[22] J. Stenger, S. Inouye, D. M. Stamper-Kurn, H.-J. Miesner, A. P. Chikkatur, and W. Ketterle. Spin domains in ground-state Bose-Einstein condensates. *Nature*, 396:345, November 1999.

[23] H.-J. Miesner, D. M. Stamper-Kurn, J. Stenger, S. Inouye, A. P. Chikkatur, and W. Ketterle. Observation of metastable states in spinor Bose-Einstein condensates. *Phys. Rev. Lett.*, 82(11):2228, March 1999.

[24] D. M. Stamper-Kurn, H.-J. Miesner, A. P. Chikkatur, S. Inouye, J. Stenger, and W. Ketterle. Quantum tunneling across spin domains in a Bose-Einstein condensate. *Phys. Rev. Lett.*, 83(4):661, July 1999.

[25] J. M. McGuirk, H. J. Lewandowski, D. M. Harber, T. Nikuni, J. E. Williams, and E. A. Cornell. Spatial resolution of spin waves in an ultracold gas. *Phys. Rev. Lett.*, 89(9):090402, August 2002.

[26] A. E. Leanhardt, Y. Shin, D. Kielpinski, D. E. Pritchard, and W. Ketterle. Coreless vortex formation in a spinor Bose-Einstein condensate. *Phys. Rev. Lett.*, 90(14):140403, April 2003.

[27] H. Schmaljohann, M. Erhard, J. Kronjäger, M. Kottke, S. van Staa, L. Cacciapuoti, J. J. Arlt, K. Bongs, and K. Sengstock. Dynamics of F = 2 spinor Bose-Einstein condensates. *Phys. Rev. Lett.*, 92:040402, 2004.

[28] M.-S. Chang, C. D. Hamley, M. D. Barrett, J. A. Sauer, K. M. Fortier, W. Zhang, L. You, and M. S. Chapman. Observation of spinor dynamics in optically trapped 87Rb Bose-Einstein condensates. *Phys. Rev. Lett.*, 92:140403.

[29] H. Pu and P. Meystre. Creating macroscopic atomic Einstein-Podolsky-Rosen states from Bose-Einstein condensates. *Phys. Rev. Lett.*, 85:3987, 2000.

[30] L. You and M. S. Chapman. Quantum entanglement using trapped atomic spins. *Phys. Rev. A*, 62:052302, 2000.

[31] A. Sørensen, L.-M. Duan, J. I. Cirac, and P. Zoller. Many-particle entanglement with Bose-Einstein condensates. *Nature*, 409:63, 2001.

[32] B. Julsgaard, A. Kozhekin, and E. S. Polzik. Experimental long-lived entanglement of two macroscopic objects. *Nature*, 413:400, 2001.

[33] O. Mandel, M. Greiner, A. Widera, T. Rom, T. W. Hänsch, and I. Bloch. Controlled collisions for multi-particle entanglement of optically trapped atoms. *Nature*, 425:937, 2003.

[34] M. D. Barrett, J. A. Sauer, and M. S. Chapman. All-optical formation of an atomic Bose-Einstein condensate. *Phys. Rev. Lett.*, 87(1):010404, July 2001.

[35] T. Kuwamoto, K. Araki, T. Eno, and T. Hirano. Magnetic field dependence of the dynamics of ^{87}Rb spin-2 Bose-Einstein condensates. *Phys. Rev. A*, 69:063604, 2004.

[36] H. J. Lewandowski, J. M. McGuirk, D. M. Harber, and E. A. Cornell. Decoherence-driven cooling of a degenerate spinor Bose gas. *Phys. Rev. Lett.*, 91:240404, 2003.

[37] M. Erhard, H. Schmaljohann, J. Kronjäger, K. Bongs, and K. Sengstock. Bose-Einstein condensation at constant temperature. *cond-mat/*, 0402003, 2004.

[38] A. Sinatra, C. Lobo, and Y. Castin. Classical-field method for time dependent Bose-Einstein condensed gases. *Phys. Rev. Lett.*, 87:210404, 2001.

[39] B. Jackson and E. Zaremba. Modeling Bose-Einstein condensed gases at finite temperatures with n-body simulations. *Phys. Rev. A*, 66:033606, 2002.

[40] K. Gòral, M. Gajda, and K. Rzążewski. Thermodynamics of an interacting trapped Bose-Einstein gas in the classical field approximation. *Phys. Rev. A*, 66:051602, 2002.

[41] D. A. W. Hutchinson S. A. Morgan, M. Rusch and K. Burnett. Quantitative test of thermal field theory for Bose-Einstein condensates. *Phys. Rev. Lett.*, 91:250403, 2003.

[42] T. Nikuni and A. Griffin. Frequency and damping of hydrodynamic modes in a trapped Bose-condensed gas. *Phys. Rev. A*, 69:023604, 2004.

[43] K. E. Strecker, G. B. Partridge, and R. G. Hulet. Conversion of an atomic Fermi gas to a long-lived molecular Bose gas. *Phys. Rev. Lett.*, 91:080406, 2003.